

N 7 2 - 2 7 5 2 8

**NASA TECHNICAL
MEMORANDUM**

NASA TM X-68093

NASA TM X-68093

**CASE FILE
COPY**

**OPTIMAL SPEED SHARING CHARACTERISTICS
OF A SERIES-HYBRID BEARING**

by Lester J. Nypan, Herbert W. Scibbe, and
Bernard J. Hamrock
Lewis Research Center
Cleveland, Ohio

TECHNICAL PAPER proposed for presentation at
International Lubrication Conference sponsored by the
American Society of Mechanical Engineers and the
American Society of Lubrication Engineers
New York, New York, October 9-12, 1972

OPTIMAL SPEED SHARING CHARACTERISTICS
OF A SERIES-HYBRID BEARING

by Lester J. Nypan,* Herbert W. Scibbe, and Bernard J. Hamrock

Lewis Research Center

ABSTRACT

A series-hybrid bearing assembly consisting of a conical hydrostatic fluid-film bearing and a ball bearing is described. Computer studies are used to predict friction torque and life characteristics of a 150-millimeter ball bearing. A conical hydrostatic fluid-film bearing is designed for minimum friction and maximum speed reduction of the ball-bearing component of the series-hybrid bearing. At a thrust load of 4000 pounds and speeds corresponding to DN (bearing bore in millimeters times shaft speed in rpm) values of 3 and 4 million, ball-bearing speed may be reduced by 30 percent. This speed reduction corresponds to ball-bearing fatigue life improvement factors of 3.4 at 3 million DN and 5.9 at 4 million DN. An oil flow rate of 18.2 pounds per minute is required to maintain a fluid-film thickness of 0.001 inch in the hydrostatic bearing.

NOMENCLATURE

C_2 dimensionless turbulent friction coefficient,

$$0.0261 f_r (\rho R_1 \omega_f h_p / \mu)^{0.75} (h_L / h_p)$$

D ball-bearing bore diameter, in.

d ball diameter, in.

F thrust load, lb

\bar{F} dimensionless thrust load parameter, $2F/\pi p R_1^2$

*Professor of Engineering, San Fernando Valley State College, Northridge, California; NASA Summer Faculty Fellow in 1971.

f_r	fraction of area between R_2 and R_3 occupied by hydrostatic pocket (usually may be approximated by 1)
g	gravitational constant, 386.4 in./sec^2
h	fluid-film thickness, in.
M	friction torque, in. - lb
\overline{M}	dimensionless friction torque
M_b	ball-bearing torque, in. - lb
M_f	fluid-film bearing torque, in. - lb
M_f	dimensionless fluid-film bearing torque, $2M_f h_L \sin \theta / \pi \mu \omega_f$
m	oil mass flow rate, lb/min
N	ball-bearing speed, rpm
N_f	fluid-film bearing speed, rpm
N_s	shaft speed, rpm
p	pressure, lb/in. ²
Q	fluid flow, in. ³ /sec
\overline{Q}	dimensionless fluid-flow parameter, $6\mu Q / \pi h_L^3 p \sin \theta$
q	power loss rejected to the oil, hp
R	typical radius on fluid-film bearing, in.
R_1	inner radius of inner land, in.
R_2	outer radius of inner land, in.
R_3	inner radius of outer land, in.
R_4	outer radius of outer land, in.
Re	Reynolds number, $\rho V h / \mu$
V	bearing surface speed, in./sec
X_2	R_2 / R_1
X_3	R_3 / R_1

X_4	R_4/R_1
Z	number of balls
θ	half angle of conical hydrostatic bearing, deg
μ	fluid dynamic viscosity, lb-sec/in. ²
ρ	fluid density, lb/in. ³
ω_b	rotational speed of ball bearing, rad/sec
ω_f	rotational speed of fluid-film bearing, rad/sec
ω_s	rotational speed of shaft, $\omega_b + \omega_f$, rad/sec

Subscripts:

L	land
p	pocket

INTRODUCTION

The use of low mass hollow or drilled balls in high speed bearings, to reduce contact stress and thereby improve fatigue life, has been demonstrated with limited success in several experimental programs [1-4]. Another method for improving fatigue life of a ball bearing is to reduce its rotational speed by coupling it in series with a fluid-film bearing. This arrangement, called the series-hybrid bearing, is shown in figure 1. In the series-hybrid bearing, each bearing carries the full thrust load at part speed. The inner fluid-film bearing member rotates with the shaft at full shaft speed. The intermediate fluid-film bearing member rotates with the ball bearing inner race at some fraction of the shaft speed. The outer race of the ball bearing is mounted in a stationary housing. Oil to pressurize the fluid-film bearing is fed through the hollow shaft. Oil to lubricate and cool the ball bearing is fed under the scoop attached to the intermediate member as shown in figure 1.

At low shaft speed the inner and intermediate fluid-film bearing members rotate together at the same speed. As shaft speed increases, the intermediate member separates from the inner member by the generation of a fluid film, due to the hydrostatic pressure developed by the centrifugal force of the oil. At separation, there is a differential in speed between the inner member of the fluid-film bearing and intermediate member attached to the inner race of the ball bearing. This speed differential results in a lower speed for the ball bearing and thereby reduces ball centrifugal force (and thus contact stress) at the outer race. An experimental study [5] was conducted with a combination self-acting journal and hydrostatic thrust fluid-film bearing coupled to a 75-millimeter-bore ball bearing. The lowest speed ratio (ball bearing inner-race speed to shaft speed) obtained in the study of reference 5 was 0.67, which corresponded to a reduction in ball-bearing DN (bearing bore in millimeters times shaft speed in rpm) of one-third.

The objectives of this investigation are (1) to predict the operating characteristics of an optimally configured series-hybrid bearing at specific operating conditions, and (2) to determine whether the ball-bearing life would be sufficiently improved to warrant fabrication and experimental operation at thrust loads to 4000 pounds and DN values to 4 million. A more complete analysis of this optimally configured series-hybrid bearing is reported in reference 6.

The bearing system was optimized by (1) specifying ball diameter and complement for maximum life and speed reduction of a 150-millimeter ball bearing, and (2) specifying a conical hydrostatic fluid-film bearing configuration and dimensions to maximize speed reduction of the ball bearing.

ANALYSIS

A characteristic of the operation of a series-hybrid fluid-film ball bearing system is that the torque causing rotation of the ball bearing is the friction torque transmitted through the fluid-film bearing. As each component rotates under the action of the same torque, the speed of each bearing depends on the torque-speed relation of that component. Success of the series-hybrid bearing concept in reducing the speed of the ball-bearing component depends on the fluid-film bearing operating at an appreciable fraction of shaft speed.

To produce a long life series-hybrid bearing, factors that affect the life of the ball-bearing component must be considered. Ball-bearing friction torque is also of importance as the friction torque will determine the speed reduction that may be obtained from the fluid-film bearing.

Ball-Bearing Characteristics

A computer program [7] was used to study the life and torque characteristics of a 150-millimeter angular contact ball bearing which was the rolling-element portion of the series-hybrid bearing. Bearing running conditions investigated were speed parameter values of 3 and 4 million DN and thrust loads of 1000 pounds, as representative of a cruise condition of aircraft turbine engine operation, and 4000 pounds, as representative of a maximum load or takeoff condition of operation.

The rolling-element bearing design was optimized with respect to the maximum ball complement (Z) and the largest ball diameter (d) that could be accommodated within a 150-millimeter bore ball bearing envelope. Restrictions on these two variables were, (1) the largest number of balls that could be fitted into the bearing and still maintain a minimum cage web

thickness of 0.100 inch between the ball pockets at the pitch diameter; and, (2) limit the maximum ball diameter to less than 60 percent of the radial cross section ($\text{o.d.} - \text{i.d.} / 2$) to ensure adequate race stiffness and strength. The number of balls was varied from 22 to 38, whereas ball diameter ranged from 0.500 to 0.875 inch.

Friction torque is not strongly affected by ball diameter, but is influenced by bearing load and speed conditions. Torque decreases slightly with the number of balls at the 4000 pound load condition, but increases slightly with the number of balls at the 1000 pound load. In the final analysis 22-0.875-inch diameter balls were selected as optimum for the 150-millimeter ball bearing. The inner and outer raceway curvatures were both 0.52. Figure 2 shows bearing torque variations as a function of speed for thrust loads of 1000 and 4000 pounds.

At the same load and speed condition, bearing fatigue (L_{10}) life increases with increasing ball diameter and number. Figure 3 shows the 150-millimeter bearing fatigue life in hours as a function of DN for thrust loads of 1000 to 4000 pounds.

Ball-bearing friction torque values are of considerable interest as they will strongly influence the success of the hybrid bearing concept in reducing ball-bearing speed. To evaluate the accuracy of torque predictions, the computer program [7] was used to calculate torque values for bearings experimentally evaluated by Barwell and Hughes [8]. These bearings were 127-millimeter bore, and had 19-0.500-inch diameter balls, and were oil jet lubricated. The bearings were operated at thrust loads from 500 to 4000 pounds and a constant radial load of 600 pounds, at shaft speeds up to 11 000 rpm (DN value of 1.4 million). Comparison of mea-

sured and computed friction torque for these bearings indicated that the computer program [7] predicts values appreciably higher than measured values. The largest differences were, however, less than an order of magnitude. Experimental data of Winn and Badgley [9] on the friction torque of 120-millimeter ball bearings, when compared to computed torque values, were lower but within an order of magnitude variation when differences in oil flow, viscosity, and bearing size are taken into account.

Winn and Badgley [9] presented measured and calculated values of power loss for a 120-millimeter bore ball bearing. Bearing thrust load ranged from 250 to 2840 pounds at speeds from 4000 to 10 000 rpm (0.48 to 1.20 million DN). Bearing calculated power loss was based on an empirical equation developed by Nemeth, Macks, and Anderson [10] which gives power loss rejected to the oil. Reference 9 gives the effect of a 2-gpm-flow rate on bearing friction torque measured as increasing the power losses over a bearing with a 1-gpm flow rate by 30 and 50 percent, respectively, for the 8000- and 10 000-rpm bearing speeds. Before the power loss for the 150-millimeter ball bearing in the present study can be determined by the method presented [10], a viscosity-diameter correction factor of 1.61 must be applied to account for differences in oil viscosity and bearing size. When increases of 30- and 50-percent are also applied, as noted above, to account for an oil flow rate of 2 gpm, the factor becomes 2.1 and 2.4, respectively, for the 8000- and 10 000-rpm cases reported. When these factors are applied to the average of the power losses reported for these speeds, and the result converted to friction torque, the torque values are 29.6 inch-pounds at 8000 rpm and 57.5 inch-pounds at 10 000 rpm. In view of the difficulty in replicating all of these factors and the

difficulty in predicting bearing friction torques, these values seem to adequately check the predicted bearing torques of figure 2.

Fluid-Film Bearing Characteristics

A fluid-film bearing having a low torque-rotational speed characteristic is required to match the torque of the ball bearing and thereby obtain an appreciable reduction in ball bearing speed.

While a thrust load is the primary load in this application, the bearing must also have some radial load capacity. To avoid the complexity and reduce the friction of separate thrust and journal bearings, a conical hydrostatic bearing was selected as the fluid-film bearing component of the series-hybrid bearing system. A schematic of a conical hydrostatic bearing, indicating the location of the bearing land and pocket radii, is shown in figure 4. The conical hydrostatic bearing will provide both thrust and radial load capacity. It can also be a useful component in an experimental apparatus as the fluid-film thickness can be simply controlled by adjusting the flow rate to the bearing.

Minimum friction conical hydrostatic bearings have been the subject of a recent study [11]. This has resulted in the following expression for friction torque within the turbulent regime:

$$M_f = \frac{\pi \mu \omega_f R^4}{2 h_L \sin \theta} \left[X_4^4 - X_3^4 + X_2^4 - 1 + 0.0261 \left(\frac{\rho R_1 \omega_f h_p}{\mu} \right)^{0.75} f_r \frac{h_L}{h_p} (X_3^{4.75} - X_2^{4.75}) \right] \quad (1)$$

Preliminary calculations indicate that a hydrostatic bearing with a speed of 1700 rpm and using a Type II ester fluid (MIL-L23699) at 200° F will be operating within the turbulent regime ($Re > 1000$). The hydrostatic bearing

dimensions selected are compatible with the 150-millimeter ball bearing.

Reference 11 describes methods for the selection of bearing geometry to minimize friction torque. These methods are applied here to specify a minimum friction conical hydrostatic bearing to function as the fluid-film part of the series-hybrid bearing system operating at a shaft speed equivalent to a DN of 3 million (for a ball bearing) while supporting a 4000-pound thrust load. Operating characteristics of the bearing at a 1000-pound thrust load and at bearing DN values of 3 and 4 million are also considered.

Oil may be fed to the bearing from the shaft centerline and pressure developed by centrifugal action. Centrifugal pressure available is

$$p = \frac{\rho \omega_s^2 R^2}{2g} \quad (2)$$

From preliminary layouts, it appears that the innermost fluid-film bearing radius that will permit the largest shaft possible through the bearing, and still mate with the 150-millimeter ball bearing will be $R_1 = 2.81$ inches. If a Type II ester fluid (MIL-L23699) is used, the density ρ will be 0.035 pound/in.³ at 200° F. A centrifugal pressure of 1530 psi will then be available at a speed of 20 000 rpm (DN = 3 million). This is sufficient to support loads of 4000 pounds and provide compensation for misalignment and varying loads.

High thrust load condition (4000 lb). - The dimensionless thrust parameter to be used in selecting a minimum friction bearing [11] is

$$F = \frac{2F}{\pi p R_1^2} \quad (3)$$

Preliminary calculations have suggested a value of $p = 645$ psi be used in equation (3). This allows a larger fraction of the available pressure for

compensation than is suggested by Ling [12] for maximum stiffness. Stiffness will increase if load rises above the 4000 pounds considered. This gives a thrust parameter \bar{F} of 0.5. The friction torque M_f and bearing dimensions for a minimum friction conical hydrostatic bearing are determined from reference 11 as functions of the dimensionless flow parameter

$$\bar{Q} = \frac{6\mu Q}{\pi p h_L^3 \sin \theta} \quad (4)$$

Table I shows the predicted friction torque M_f as a function of flow parameter \bar{Q} for combinations of minimum fluid-film thickness h_L and fluid-film bearing speeds N_f . Minimum fluid-film thicknesses selected for consideration were $h_L = 0.002, 0.001, \text{ and } 0.0005$ inch. Fluid-film bearing speeds N_f were calculated from ω_f indicated in the hydrostatic pocket friction parameter

$$C_2 = 0.0261 \left(\frac{\rho R_1 \omega_f h_p}{\mu} \right)^{0.75} f_r \frac{h_L}{h_p} \quad (5)$$

with values of $C_2 = 0.8, 0.4, \text{ and } 0.2$ for pocket depth, $h_p = 0.125$ inch.

This large pocket depth was selected to reduce pocket friction torque.

Table I gives values of \bar{M}_f associated with \bar{Q} values for $F = 0.5$, C_2 values specified previously, and the speed listed. Dimensionless \bar{Q} is converted to dimensional flow rate, Q , using equation (4), and using the density of $\rho = 0.035 \text{ lb/in.}^3$, for comparison with flow rates commonly encountered in bearing lubrication and cooling. Dimensionless friction torque \bar{M} is converted to dimensional friction torque, M , from

$$\bar{M} = \frac{2M_f h_L \sin \theta}{\pi \mu \omega_f R_1^4} \quad (6)$$

The half cone angle θ was taken to be 45° . The viscosity μ of the Type II ester at 200° F is $0.8 \times 10^{-6} \text{ (lb)(sec)/in.}^2$. It may be noted in table I that changing h_L from 0.002 to 0.001 inch reduces the flow Q by seven-eighths and increases the friction torque M_f fivefold. Values tabulated for the 0.002 inch fluid-film thickness indicate that flow requirements are so large as to make bearing operation at this film thickness impractical.

Table II gives optimum bearing dimensions for values of flow parameter \bar{Q} . Radii R_1 and R_2 are those of the inner land, while R_3 and R_4 are those of the outer land (fig. 4). As was noted [11], bearing dimensions are insensitive to changes in the hydrostatic pocket friction parameter C_2 so that only one set of bearing dimensions is obtained. For a given thrust load then, bearing dimensions depend only on flow parameter \bar{Q} and the single table of dimensions is sufficient to specify minimum friction bearings for the assumed design conditions. Figure 5 shows the relative proportions of these bearings. These range from the configuration of $\bar{Q} = 20$ where the hydrostatic pocket is shrunk into what is practically a line fed hydrostatic pad to the configuration of $\bar{Q} = 1000$ where the lands have diminished to less than 0.01 inch.

Low thrust load condition (1000 lb). - The relation among flow, thrust load, and minimum fluid-film thickness may be obtained [11] from

$$Q = \frac{\pi p h_L^3 \sin \theta}{6\mu} \left(\frac{1}{\ln \frac{R_2}{R_1}} + \frac{1}{\ln \frac{R_4}{R_3}} \right) \quad (7)$$

and

$$F = \frac{\pi p}{2} (R_4^2 + R_3^2 - R_2^2 - R_1^2) \quad (8)$$

or

$$Q = \frac{F h_L^3 \sin \theta}{3\mu (R_4^2 + R_3^2 - R_2^2 - R_1^2)} \left(\frac{1}{\ln \frac{R_2}{R_1}} + \frac{1}{\ln \frac{R_2}{R_3}} \right) \quad (9)$$

For a given bearing and lubricant $Q = k F h_L^3$ where k is a constant for the bearing and lubricant. At the 4000-pound thrust load and design flow rate, the film thickness and friction torque have been determined. At the 1000-pound thrust load and the same design flow rate, the minimum film thickness is then 1.59 times the fluid-film thickness for the 4000-pound thrust load. Friction torque may then be calculated from equation (1).

Predicted Speed Share and Life Improvement Factors

After determining the friction torque-speed characteristics for the ball bearing and the fluid-film bearing, the speed sharing performance of the series-hybrid bearing may be predicted. From this speed sharing, the life improvement of the series-hybrid bearing over the unassisted ball bearing is determined.

Predicted speed share. - The sum of the speeds of the fluid-film bearing will be equal to the shaft speed, that is, $\omega_s = \omega_f + \omega_b$. The torque-speed characteristics of the two bearing components of the series-hybrid bearing may be conveniently compared by plotting fluid-film bearing torque, M_f , as a function of fluid-film bearing speed, ω_f , and ball-bearing torque, M_b , as a function of ball-bearing speed, $\omega_b = \omega_s - \omega_f$, on the

same axes. The operating speed of the fluid-film bearing is then readily determined as the speed consistent with the common torque $M_f = M_b$, operating to drive the bearings at the speeds ω_f and ω_b .

Figure 6 shows torque-speed curves for the five fluid-film bearings designs of figure 5 operating at 4000-pound thrust load with fluid film thicknesses of 0.001 and 0.0005 inch. Values of friction torque from table I are plotted as functions of fluid-film bearing speed. Figure 6(a) shows results for a hydrostatic pocket depth of 0.125 inch, and the 0.001-inch fluid-film thickness. Figure 6(b) shows results for a hydrostatic pocket depth of 0.125 inch, and 0.0005-inch fluid-film thickness. Friction torque curves for the 150-millimeter ball bearing in a series-hybrid bearing operating at shaft speeds of 20 000 and 26 667 rpm (DN = 3 and 4 million for the 150-mm bearing) and at 4000 pound thrust load are also plotted on figure 6. Points of intersection indicate operating conditions of equal torque and compatible bearing speeds for the series-hybrid bearing components.

Figure 6 indicates that substantial speed ratios (speed ratio = ball bearing speed/shaft speed) may be obtained for this series-hybrid bearing design. Figure 6(a) for example, shows that at a \bar{Q} value of 30 and a shaft speed of 20 000 rpm (3 million DN) the fluid-film bearing operates at 6400 rpm and the ball bearing at 13 600 rpm. At a \bar{Q} value of 30 and 26 667 rpm (4 million DN) shaft speed the fluid-film and ball bearings speeds are 8000 and 18 667 rpm, respectively. At the 3 million DN shaft speed the speed ratio for the ball bearing is therefore 0.68, whereas at 4 million DN shaft speed the speed ratio is 0.70. Table III(a) gives the values of the predicted speed ratios for bearings having \bar{Q} values of 20, 30, 70, and 100 at the two shaft speeds for a 4000-pound thrust load.

Figure 7 shows torque-speed curves similar to those of figure 6 for the 1000-pound thrust load condition. Predicted speed ratios for this load condition are given in table III(b).

In the analysis of this series-hybrid bearing, operation of the fluid-film bearing at a film thickness of 0.0005 inch may be marginal, since the effects of thermal growth or axial deflection under applied thrust have not been taken into account. Also minute debris not filtered out of the oil lubrication system may not permit bearing operation at this low value of film thickness. An increase in operating film thickness from 0.001 to 0.002 inch requires an eight-fold increase in oil flow for the same bearing load and speed conditions. Because of this increase in oil flow required through the fluid-film bearing, a 0.002 inch film thickness is therefore impractical for this application. Best estimate of a film thickness for the bearing operating conditions considered herein is about 0.001 inch. The 18.2-pound per minute oil flow required for the two shaft speeds at the 4000-pound thrust load condition is comparable to oil flows used to cool and lubricate bearings in present-day gas-turbine aircraft engines.

Life improvement factors. - The potential increase in ball bearing fatigue life due to a reduction in the effective DN value can be seen from figure 3. With the 150-millimeter-bore ball bearing operating at a DN of 3 million and 4000-pound thrust load, its expected L_{10} fatigue life is 520 hours. If the same bearing is operated in a series-hybrid arrangement with a speed ratio of 0.7, its effective DN is 2.1 million and its L_{10} fatigue life is 1750 hours. The life improvement factor is $1750/520 = 3.4$. With the 4000-pound thrust load, at a DN of 4 million and speed ratio of 0.7, the L_{10} life of 120 hours would improve to 710 hours at an effective DN of 2.8 million for a life improvement factor of 5.9.

In the 1000-pound thrust load cases, the speed ratio of 0.7 again provides effective DN values of 2.1 and 2.8 million for shaft speeds corresponding to a DN of 3 and 4 million with life improvement ratios of 3.9 and 7.1.

CONCLUSIONS

A series-hybrid fluid-film bearing may be constructed to reduce ball bearing speed by 30 percent. Relatively moderate flow rates are required for its operation. At a 4000-pound thrust load and shaft speeds corresponding to speed parameter DN values of 3 and 4 million for a 150-millimeter ball bearing, a flow of 18.2 pounds per minute is required to maintain a fluid-film thickness of 0.001 inch for the optimum bearing dimensions. The resulting life improvement factors are 3.4 and 5.9 for DN values of 3 and 4 million, respectively.

REFERENCES

1. Coe, H. H., Parker, R. J. and Scibbe, H. W., "Evaluation of Electron-Beam Welded Hollow Balls for High-Speed Ball Bearings," Journal of Lubrication Technology, Vol. 93, No. 1, Jan. 1971, pp. 47-59.
2. Coe, H. H., Scibbe, H. W. and Anderson, W. J., "Evaluation of Cylindrically Hollow (Drilled) Balls in Ball Bearings at DN Values to 2.1 Million," TN D-7007, 1971, NASA, Cleveland, Ohio.
3. Holmes, P. W., "Evaluation of Drilled-Ball Bearings at DN Values to Three Million. I - Variable Oil Flow Tests," CR-2004, 1972, NASA, Washington, D.C.
4. Holmes, P. W., "Evaluation of Drilled-Ball Bearings at DN Values to Three Million. II - Experimental Skid Study and Endurance Tests," CR-2005, 1972, NASA, Washington, D.C.

5. Anderson, W. J., Fleming, D. P. and Parker, R. J., "The Series Hybrid Bearing - A New High Speed Bearing Concept," Journal of Lubrication Technology, Vol. 94, No. 2, Apr. 1972, pp. 117-124.
6. Nypan, L. J., Hamrock, B. J., Scibbe, H. W. and Anderson, W. J., "Predicted Characteristics of an Optimized Series-Hybrid Conical Hydrostatic Ball Bearing," TN D-6607, 1971, NASA, Cleveland, Ohio.
7. Crecelius, W. J. and Harris, T. A., "Ultra-High-Speed Ball Bearing Analysis," NASA CR-120837, 1971, SKF Industries, Inc., King of Prussia, Pa.
8. Barwell, F. T. and Hughes, M. J., "Some Further Tests on High-Speed Ball-Bearings," Proceedings of the Institution of Mechanical Engineers, Vol. 169, No. 36, 1955, pp. 699-706.
9. Winn, L. W. and Badgley, R. H., "Development of Long Life Jet Engine Thrust Bearings," MTI-70TR44, NASA CR-72744, June 1970, Mechanical Technology, Inc., Latham, N.Y.
10. Nemeth, Z. N., Macks, E. F. and Anderson, W. J., "Investigation of 75-Millimeter-Bore Deep-Grooved Ball Bearings under Radial Load at High Speeds. II - Oil Inlet Temperature, Viscosity, and Generalized Cooling Correlation," TN 3003, 1953, NACA, Cleveland, Ohio.
11. Nypan, L. J., Hamrock, B. J., Scibbe, H. W. and Anderson, W. J., "Optimization of Conical Hydrostatic Bearing for Minimum Friction," Journal of Lubrication Technology, Vol. 94, No. 2, Apr. 1972, pp. 136-142.
12. Ling, M. T. S., "On the Optimization of the Stiffness of Externally Pressurized Bearings," Journal of Basic Engineering, Vol. 84, No. 1, Mar. 1962, pp. 119-122.

TABLE I. - FLOW AND FRICTION TORQUE FOR THREE
FLUID-FILM THICKNESSES

[Pocket depth $h_p = 0.125$ in.]

Dimen- sionless flow rate, \bar{Q}	Fluid flow, $\frac{Q}{\text{min}}$ $\frac{\text{lb}}{\text{min}}$	Dimen- sionless friction torque, \bar{M}	Fluid-film bearing torque, M_f , in. -lb	Dimen- sionless friction torque, \bar{M}	Fluid-film bearing torque, M_f , in. -lb
		$h_L = 0.002$ in.; $C_2 = 0.8$; $N_f = 5869$ rpm		$h_L = 0.002$ in.; $C_2 = 0.4$; $N_f = 2329$ rpm	
20	96.2	1.239	42.2	1.235	16.70
30	146.0	.989	33.8	.879	11.91
70	340.0	.732	25.0	.520	7.05
100	486.0	.679	23.2	.445	6.03
1000	4863.0	.571	19.5	.296	4.01

Dimen- sionless flow rate, \bar{Q}	Fluid flow, $\frac{Q}{\text{min}}$ $\frac{\text{lb}}{\text{min}}$	Dimen- sionless friction torque, \bar{M}	Fluid-film bearing torque, M_f , in. -lb	Dimen- sionless friction torque, \bar{M}	Fluid-film bearing torque, M_f , in. -lb
		$h_L = 0.001$ in.; $C_2 = 0.8$; $N_f = 14\ 789$ rpm		$h_L = 0.001$ in.; $C_2 = 0.4$; $N_f = 5869$ rpm	
20	12.1	1.239	213	1.235	84.4
30	18.2	.989	170	.879	60.0
70	42.6	.732	126	.520	35.5
100	60.8	.679	117	.445	30.4
1000	608.0	.571	98	.296	20.2

Dimen- sionless flow rate, \bar{Q}	Fluid flow, $\frac{Q}{\text{min}}$ $\frac{\text{lb}}{\text{min}}$	Dimen- sionless friction torque, \bar{M}	Fluid-film bearing torque, M_f , in. -lb	Dimen- sionless friction torque, \bar{M}	Fluid-film bearing torque, M_f , in. -lb
		$h_L = 0.0005$ in.; $C_2 = 0.4$; $N_f = 14\ 789$ rpm		$h_L = 0.0005$ in.; $C_2 = 0.2$; $N_f = 5869$ rpm	
20	1.52	1.235	426	1.232	167.0
30	2.28	.879	303	.824	112.6
70	5.32	.520	179	.413	56.4
100	7.60	.445	153	.328	44.8
1000	75.99	.296	102	.158	21.6

TABLE II. - OPTIMUM BEARING DIMENSIONS FOR MINIMUM FRICTION

TORQUE (FOR ALL VALUES OF C_2 AND $\bar{F} = 0.5$)

Dimensionless flow rate, \bar{Q}	Inner radius of inner land, R_1 , in.	Outer radius of inner land, R_2 , in.	Inner radius of outer land, R_3 , in.	Outer radius of outer land, R_4 , in.
20	2.812	3.105	3.110	3.440
30	↓	3.012	3.127	3.338
70		2.899	3.138	3.225
100		2.874	3.141	3.200
1000		2.818	3.144	3.149

TABLE III. - PREDICTED SPEED RATIOS (BALL BEARING SPEED/SHAFT SPEED)

[Pocket depth $h_p = 0.125$ in.]

(a) 4000-lb thrust load

Dimen- sionless flow rate, \bar{Q}	Fluid flow, $\frac{Q}{\text{lb}} \frac{\text{min}}$	Shaft speed, N_s , rpm		Fluid flow, $\frac{Q}{\text{lb}} \frac{\text{min}}$	Shaft speed, N_s , rpm	
		20 000	26 667		20 000	26 667
		Speed ratio			Speed ratio	
	$h_L = 0.001 \text{ in.}$			$h_L = 0.0005 \text{ in.}$		
20	12.1	0.75	0.78	1.52	0.86	0.87
30	18.2	.68	.70	2.28	.80	.81
70	42.6	.59	.62	5.32	.67	.70
100	60.8	.57	.60	7.60	.63	.66

(b) 1000-lb thrust load

Dimen- sionless flow rate, \bar{Q}	Fluid flow, $\frac{Q, \text{ lb}}{\text{min}}$	Shaft speed, N_s , rpm		Fluid flow, $\frac{Q, \text{ lb}}{\text{min}}$	Shaft speed, N_s , rpm	
		20 000	26 667		20 000	26 667
		Speed ratio			Speed ratio	
	$h_L = 0.00159 \text{ in.}$			$h_L = 0.00079 \text{ in.}$		
20	12.1	0.72	0.71	1.52	0.83	0.83
30	18.2	.61	.67	2.28	.78	.78
70	42.6	.60	.60	5.32	.67	.67
100	60.8	.57	.60	7.60	.64	.64

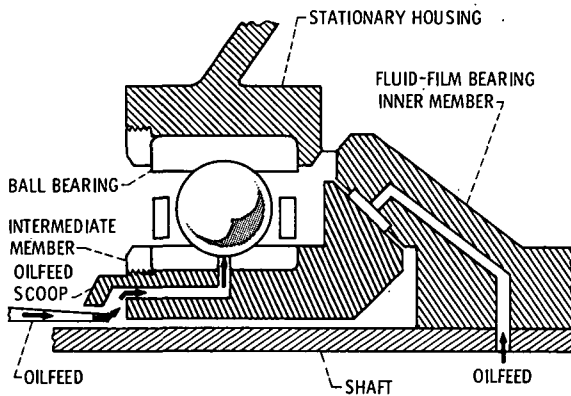


Figure 1. - Schematic diagram of a typical series-hybrid fluid-film, rolling element bearing.

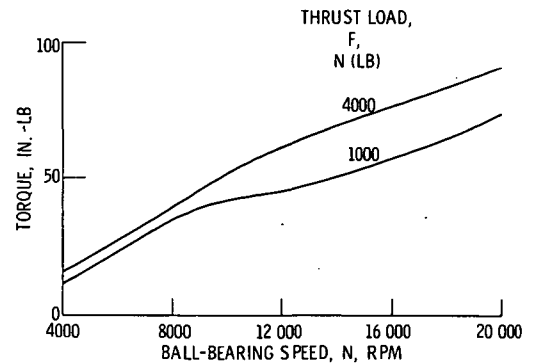


Figure 2. - Computed torque-speed relation for a 150-millimeter-bore bearing based on analysis of reference 7. Ball diameter, 0.875 inch, pitch diameter, 7.358 inches.

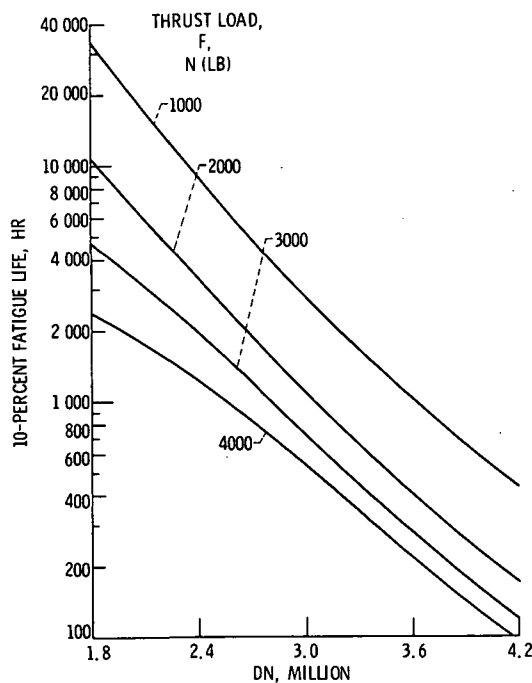
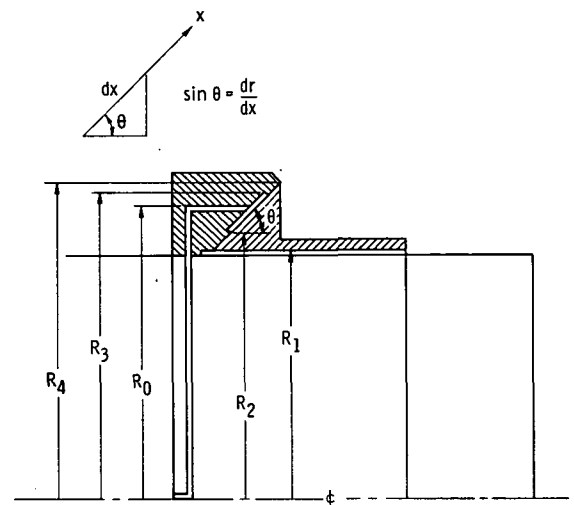
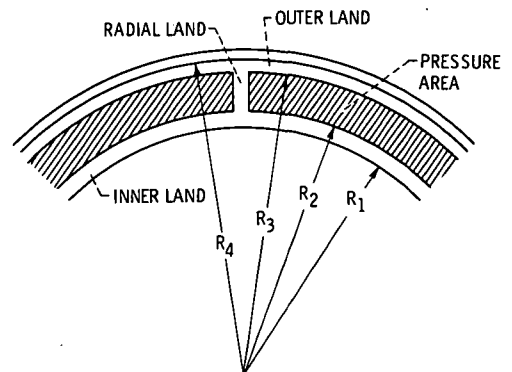


Figure 3. - Theoretical fatigue life of thrust-loaded 150-millimeter-bore ball bearing, based on analysis of reference 7. (Data from ref. 5.)



(a) SECTION VIEW.



(b) FRONT VIEW.

Figure 4. - Schematic diagrams of conical hydrostatic bearing design.

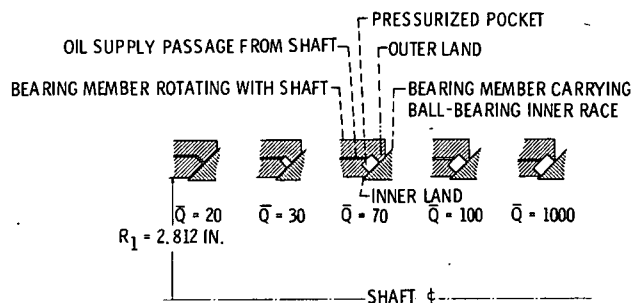


Figure 5. - Bearing proportions for values of dimensionless flow rate \bar{Q} . Inner radius of inner land $R_1 = 2.812$ inches.

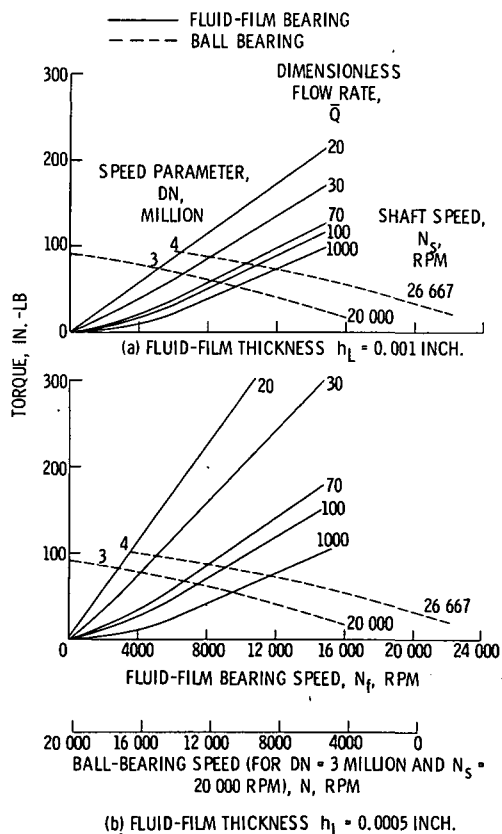


Figure 6. - Torque as a function of speed for a series-hybrid bearing. Thrust level, $F = 4000$ pounds, pocket depth $h_p = 0.125$ inch.

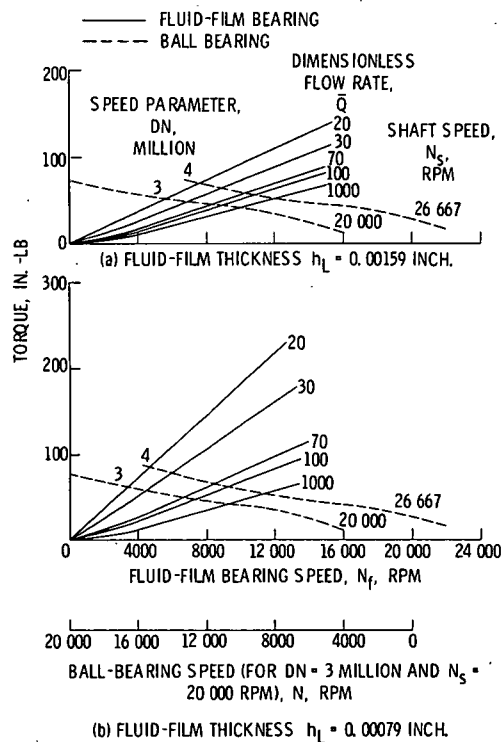


Figure 7. - Torque as a function of speed for a series-hybrid bearing. Thrust load $F = 1000$ pounds, pocket depth $h_p = 0.125$ inch.